Tropomodulin 1 Regulation of Actin Is Required for the Formation of Large Paddle Protrusions Between Mature Lens Fiber Cells

Catherine Cheng,[1] Roberta B. Nowak,[1] Sondip K. Biswas,[2] Woo-Kuen Lo,[2] Paul G. FitzGerald,[3] and Velia M. Fowler[1]

[1]Department of Cell and Molecular Biology, The Scripps Research Institute, La Jolla, California, United States
[2]Department of Neurobiology, Morehouse School of Medicine, Atlanta, Georgia, United States
[3]Department of Cell Biology and Human Anatomy, University of California, Davis, California, United States

Correspondence: Velia M. Fowler, Department of Cell and Molecular Biology, MB114, The Scripps Research Institute, 10550 N. Torrey Pines Road, La Jolla, CA 92037, USA; velia@scripps.edu.

Submitted: May 17, 2016
Accepted: June 25, 2016

Citation: Cheng C, Nowak RB, Biswas SK, Lo W-K, FitzGerald PG, Fowler VM. Tropomodulin 1 regulation of actin is required for the formation of large paddle protrusions between mature lens fiber cells. *Invest Ophthalmol Vis Sci*. 2016;57:4084–4099. DOI:10.1167/iovs.16-19949

Purpose. To elucidate the proteins required for specialized small interlocking protrusions and large paddle domains at lens fiber cell tricellular junctions (vertices), we developed a novel method to immunostain single lens fibers and studied changes in cell morphology due to loss of tropomodulin 1 (Tmod1), an F-actin pointed end–capping protein.

Methods. We investigated F-actin and F-actin–binding protein localization in interdigitations of *Tmod1*$^{+/+}$ and *Tmod1*$^{-/-}$ single mature lens fibers.

Results. F-actin–rich small protrusions and large paddles were present along cell vertices of *Tmod1*$^{+/+}$ mature fibers. In contrast, *Tmod1*$^{-/-}$ mature fiber cells lack normal paddle domains, while small protrusions were unaffected. In *Tmod1*$^{+/+}$ mature fibers, Tmod1, β2-spectrin, and α-actinin are localized in large puncta in valleys between paddles; but in *Tmod1*$^{-/-}$ mature fibers, β2-spectrin was dispersed while α-actinin was redistributed at the base of small protrusions and rudimentary paddles. Fimbrin and Arp3 (actin-related protein 3) were located in puncta at the base of small protrusions, while N-cadherin and ezrin outlined the cell membrane in both *Tmod1*$^{+/+}$ and *Tmod1*$^{-/-}$ mature fibers.

Conclusions. These results suggest that distinct F-actin organizations are present in small protrusions versus large paddles. Formation and/or maintenance of large paddle domains depends on a β2-spectrin–actin network stabilized by Tmod1. α-Actinin–crosslinked F-actin bundles are enhanced in absence of Tmod1, indicating altered cytoskeleton organization. Formation of small protrusions is likely facilitated by Arp3-branched and fimbrin-bundled F-actin networks, which do not depend on Tmod1. This is the first work to reveal the F-actin–associated proteins required for the formation of paddles between lens fibers.

Keywords: interdigitations, eye, spectrin, actinin, paddles

The eye lens is a transparent and avascular organ that is responsible for fine focusing of light onto the retina. The lens is composed of a bulk of fiber cells covered by an anterior monolayer of epithelial cells and enclosed by a thin collagenous capsule.[1] Equatorial epithelial cells continuously proliferate and differentiate into newly formed hexagonal fiber cells that elongate several hundredfold[2,3] and undergo a maturation process including organelle loss and compaction to minimize light scattering.[4,5] Lens fiber cells are tightly apposed to neighboring fiber cells, connected by membrane interdigitations that become progressively more elaborate with maturation (radial depth) to form complex interfaces.[6–10] Elegant, classic electron microscopy studies have revealed that a variety of interlocking membrane protrusions and domains (balls and sockets, protrusions, paddles, tongue-and-groove ridges, and square arrays) form between neighboring hexagonal fiber cells along the broad and short sides.[8–15] These elaborate interdigitations have been hypothesized to be important for maintaining lens fiber cell adhesive interactions and mechanical integrity.[7,16]

Ball-and-socket interdigitations form along the broad sides of superficial cortical fiber cells and are composed of a small protrusion (ball) on one cell precisely fitted into the socket indentation of the neighboring cell.[9,10,12,13,17,18] Balls and sockets typically display head and neck portions with head diameters of 0.5 to 2 μm,[7,16] and while a large number of balls and sockets are observed in the superficial cortex, fewer are found in the deeper cortex.[9,10,12,13] As fiber cells continue to mature, small interlocking protrusions form between adjacent fiber cells at their tricellular junctions (vertices).[7–13,19,20] These structures are extensively distributed along the membranes of lens fiber cells that have lost their nuclei and organelles in the deeper cortex and lens nucleus.[9,10,12,13,20,21] Similar to balls and sockets, these small protrusions may also contain head and neck portions with head diameters of 0.1 to 1.5 μm.[9,10,12,13,20] In addition to small protrusions, mature fiber cells without organelles also develop large interlocking paddle domains at their vertices.[6] Paddles are highly coordinated between neighboring cells and create increased lateral complexity between fibers.[6]

Investigative Ophthalmology & Visual Science

While these diverse types of protrusions and paddles have been carefully characterized morphologically, there is limited information about their molecular composition and only hints of the molecules and mechanisms that control their formation and maintenance. Gap junction plaques are associated with balls and sockets of superficial cortical fibers in chick and monkey as well as mouse lenses, suggesting that connexins may influence their structure, and that balls and sockets may play a role in facilitating fluid and ion homeostasis and microcirculation between fiber cells as well as maintaining normal hexagonal cell shape.[16,22] Previous immunogold labeling electron microscopy studies suggest that the formation of small interlocking protrusions along the short sides of fibers near cell vertices utilizes a mechanism of plasma membrane invagination similar to clathrin-AP2–mediated endocytic pit formation,[20,23–27] and this process is hypothesized to be mediated by Arp2/3 (actin-related protein 2/3)-driven actin polymerization.[20] In *Efna5*$^{-/-}$ lenses, the formation of large globules between mature fibers has been suggested to be due to a breakdown of interlocking protrusions,[28] indicating that cell–cell adhesion through Eph–ephrin signaling may be required to maintain lens fiber cell protrusion morphologies. Recent studies have localized aquaporin-0 and N-cadherin to small protrusions at vertices in mature fiber cells,[7,28] suggesting that aquaporin-0 and N-cadherin may be required for normal formation of protrusions at fiber cell vertices. While the loss of beaded intermediate filaments due to deletion of CP49 or filensin does not affect the initial formation of small protrusions and large paddles between lens fibers, the innermost fiber cells lose their large paddles and associated protrusions, suggesting that the beaded intermediate filament network is needed to maintain these complex structures during fiber cell maturation after organelle loss.[29]

The ability to determine the molecular composition of fiber cell interlocking protrusions and their pathway for assembly and morphogenesis is confounded by the complex three-dimensional (3D) morphology and close apposition of lens fiber cell membranes, making it impossible to distinguish whether components are located in the protruding region or the complementary concave region of the interlocking membrane domains without utilization of technically challenging immunogold labeling electron microscopy approaches. This is made even more challenging by the changing patterns of fiber cell protrusions during maturation, as well as difficulty in locating protrusion types with respect to the locations of fiber cells in the lens. To overcome these challenges, we have developed a novel approach to isolate single fiber cells at different stages of maturation from different depths in the lens, followed by immunofluorescence labeling and visualization by confocal fluorescence microscopy. This approach has allowed us not only to begin to define the actin cytoskeletal composition of small protrusion domains versus large paddle domains in fiber cells at different stages of maturation, but also to determine how this cytoskeletal composition is perturbed upon deletion of tropomodulin 1 (Tmod1), an actin filament pointed end–capping protein, which we showed previously is required for normal fiber cell packing and lens stiffness.[30–32] We found that a variety of F-actin–associated proteins diagnostic of diverse F-actin architectures are selectively associated with either the interlocking small protrusions or the large paddles at the vertices of lens mature fiber cells. Further, we demonstrate that Tmod1 is essential for the formation of large paddle domains between mature fiber cells where it stabilizes the spectrin-associated F-actin network, but is without effect on F-actin organization in the small protrusions. This provides the first link between diverse F-actin structures and the morphogenesis of lens fiber cell interdigitations.

Methods

Mice

All animal procedures were performed in accordance with recommendations in the ARVO Statement for the Use of Animals in Ophthalmic and Vision Research, in the Guide for the Care and Use of Laboratory Animals by the National Institutes of Health, and under an approved protocol from the Institutional Animal Care and Use Committees at The Scripps Research Institute.

Mixed-background *Tmod1*$^{-/-}$ mice used in this study all contained a cardiac-restricted α-myosin heavy chain (*αMHC*) promoter-driven *Tmod1* transgene, as previously described.[30–35] Genotyping was as described,[34] and for brevity, mouse genotypes are referred to as *Tmod1*$^{+/+}$ and *Tmod1*$^{-/-}$. Mixed-background mice carried an endogenous mutation in the *Bfsp2/CP49* gene leading to a loss of beaded intermediate filaments in the lens.[30,36–38] We restored wild-type *Bfsp2/CP49* alleles to *Tmod1*$^{-/-}$ mice by backcrossing with wild-type C57BL6 mice, as previously described.[30] Genotyping for *Bfsp2/CP49* alleles was performed as previously described.[36] All mice used in this study were littermates that carried the *αMHC-Tmod1* transgene and wild-type *Bsfp2/CP49*.

Antibodies and Reagents

Regarding rabbit polyclonal primary antibodies, anti-pan-fimbrin was a generous gift from Paul Matsudaira (National University of Singapore),[39] and anti-human Tmod1 was prepared in our laboratory.[30] With respect to mouse monoclonal primary antibodies, anti-α-actinin (nonsarcomeric, Actn1) was from Sigma-Aldrich Corp. (A5044; St. Louis, MO, USA), anti-Arp3 was from BD Biosciences (612134; San Jose, CA, USA), anti-ezrin from Sigma-Aldrich Corp. (E8897), and anti-β2-spectrin from BD Biosciences (612563). Rat monoclonal primary antibody anti-N-cadherin was a generous gift from Dietmar Vestweber (Max-Planck-Institute for Molecular Biomedicine).[40] Secondary antibodies were Alexa-488–conjugated goat anti-rabbit (A11008; Thermo Fisher Scientific, Grand Island, NY, USA), Alexa-488–conjugated goat anti-mouse (115-545-166, minimal cross-reaction; Jackson ImmunoResearch, West Grove, PA, USA), Alexa-647–conjugated goat anti-rat (112-605-167, minimal cross-reaction; Jackson ImmunoResearch), and Alexa-647–conjugated goat anti-mouse IgG (A21236; Thermo Fisher Scientific). Rhodamine-phalloidin (R415, Thermo Fisher Scientific) was used to stain F-actin, and Hoechst 33258 (B2883; Sigma-Aldrich Corp.) stained nuclei.

Scanning Electron Microscopy

Three-month-old wild-type lenses were prepared for scanning electron microscopy (SEM) as previously described.[6] Briefly, lenses were removed from enucleated mouse eyes and immersed in 2.5% glutaraldehyde 2% formaldehyde in 0.1 M sodium cacodylate buffer at room temperature for 30 minutes to 1 hour. Lenses were then bisected along the visual axis and allowed to continue fixing overnight. After dehydration through ethanol and acetone, lenses were critical point dried. After critical point drying, lenses were split into quarters along the anterior–posterior axis, yielding a freshly fractured surface that revealed a surface spanning a complete equatorial lens radius. Imaging was conducted with a Phillips XL30 TMP scanning electron microscope (FEI Company, Eindhoven, The Netherlands).

To observe interlocking protrusions and paddles along the short sides of fiber cells, freshly isolated lenses from 2-month-old *Tmod1*$^{+/+}$ and *Tmod1*$^{-/-}$ mice were fixed in 2.5%

glutaraldehyde in 0.1 M sodium cacodylate buffer, pH 7.3, at room temperature for 48 to 72 hours. Each lens was properly oriented and fractured in an anterior–posterior orientation with a sharp razor blade to expose the longitudinal features of the fiber cell short sides along the anterior, equatorial, and posterior regions of the lens. Lens halves were then postfixed in 1% aqueous OsO_4 for 1 hour at room temperature, dehydrated in graded ethanol, and dried in a Samdri-795 critical point dryer (Tousimis, Inc., Rockville, MD, USA). Lens halves were mounted on specimen stubs and coated with gold/palladium in a Hummer 6.2 sputter coater (Anatech, Inc., Union City, CA, USA). Micrographs were taken with a JEOL 820 scanning electron microscope at 10 kV (JEOL, Tokyo, Japan). The lens nucleus was used as a reference to determine the location of images taken and to ensure that images were from comparable areas of different lenses (i.e., comparable regions were located based on measurements from the center outward).

Immunostaining of Frozen Sections

Freshly enucleated eyes were collected from 6-week-old mice. A small opening made at the corneal–scleral junction facilitated fixative penetration. Eyeballs were then fixed for 4 hours in 1% paraformaldehyde in PBS at 4°C. After fixation, samples were washed in PBS, cryoprotected in 30% sucrose, frozen in optimal cutting temperature (OCT) medium (Sakura Finetek, Torrance, CA, USA), and stored at −80°C until sectioning. Frozen sections (12 μm thick) were collected with a Leica CM1950 cryostat (Wetzlar, Germany). Immunostaining of lens sections was conducted as previously described.[31,32] ProLong Gold antifade reagent (Thermo Fisher Scientific) was used to mount the slides, and images were collected using a Zeiss LSM780 confocal microscope (Oberkochen, Germany). Frozen sections with cross-sectionally oriented fiber cells near the lens equator were identified based on the thickness of the lens epithelium.[31] Staining was repeated on three samples from different mice for each genotype, and representative data are shown.

Immunostaining of Fiber Cell Bundles and Single Lens Fiber Cells

Freshly dissected lenses were collected from 6-week-old mice. Lenses were carefully decapsulated with fine forceps, leaving the bulk mass of fibers. Decapsulated lenses were fixed in 1% paraformaldehyde in PBS overnight at 4°C. After fixation, lenses were cut into quarters using a sharp scalpel along the anterior–posterior axis. Lens quarters were postfixed in 1% paraformaldehyde in PBS for 15 minutes at room temperature and then washed two times briefly with PBS. Lens quarters were then permeabilized and blocked using 3% normal goat serum, 3% bovine serum albumin, and 0.3% Triton X-100 in PBS for 1 hour at room temperature. After blocking, lens quarters were immersed in primary antibody diluted with blocking solution overnight at 4°C. Then, samples were washed three times, 5 minutes per wash, with PBS. Lens quarters were incubated in secondary antibodies diluted in blocking solution for 3 hours at room temperature, followed by washing (four times, 5 minutes per wash) with PBS. Lens quarters were stored in ProLong Gold antifade reagent at 4°C until imaging. Images and Z-stacks with 0.2-μm steps were collected of single fiber cells or small bundles of fibers from lens quarters using a Zeiss LSM780 confocal microscope. Fiber cell morphology and cell location in relation to the bulk lens quarter were used to approximate the maturity of imaged fiber cells. Staining was repeated on at least three lenses from three different mice for each genotype, and representative data are shown.

Image Analysis

Z-stack confocal images were analyzed using Volocity 6.3 (PerkinElmer, Waltham, WA, USA). Noise reduction using the fine filter was applied to all Z-stacks in all channels. The Extended Focus function in Volocity was used to flatten Z-stacks into a single image. For fluorescence intensity heat maps, single optical sections from Z-stacks were separated into individual channels (16-bit grayscale images), and then heat maps were generated in ImageJ using the HeatMap Histogram plug-in (http://www.samuelpean.com/heatmap-histogram/ [in the public domain]). For tortuosity and cell neck width measurements, we evaluated single optical sections of single fibers stained with rhodamine-phalloidin to outline cell contours from 9 *Tmod1*$^{+/+}$ and 9 *Tmod1*$^{-/-}$ mice. Using ImageJ, we located the fiber cell edges using the Find Edges function and used the Wand Tool (Mode: Legacy; Tolerance: 5.0) to measure the length of one of the curved edges of each fiber cell in pixels. Tortuosity was calculated as the contour length of the cell edge divided by the straight end-to-end distance along the fiber measured through the center of each fiber. Fiber cell segments 42 μm in length were used for measurements. Cell neck width across each fiber at the concave region was measured using the Line Tool. Three measurements of cell neck width were averaged for each fiber cell. The average, standard error, and statistical significance were calculated and plotted in Excel (Microsoft, Redmond, WA, USA). Statistical significance was determined using the Student's *t*-test, and *P* values less than 0.01 were considered statistically significant.

Results

F-Actin Is Associated With Large Paddles and Small Protrusions at Fiber Cell Interlocking Domains

Classic electron microscopy studies have described the complex interface between differentiating and maturing lens fiber cells characterized by specialized membrane interdigitations,[6,8–10,12,13] which is shown here by SEM (Figs. 1A–D), as in our previous study.[6] Newly formed wild-type fiber cortical cells are straight with small protrusions along the short sides and balls and sockets in the middle of the broad sides (Fig. 1B, cells viewed from the short-side edge). As fiber cells differentiate, increased small protrusions appear along their short sides (Fig. 1C, top-down view of the broad sides), with mature fiber cells developing elaborate large interlocking paddles decorated with small protrusions (Fig. 1D, top-down view of the broad sides). In small bundles of *Tmod1*$^{+/+}$ lens fibers fixed and stained with phalloidin, we observed that F-actin is enriched at the interfaces between cortical (Fig. 1E), differentiating (Fig. 1F), and mature fibers (Fig. 1G). F-actin appears along the membrane of fiber cells and is present in regions of large paddles as well as small protrusions, outlining cell contours, but the precise location of F-actin with respect to the paddles or protrusions is unclear due to the complex geometry of the membrane interfaces. For clarity, a cartoon of mature fiber cells indicating the morphologic features of mature fiber cells (large paddles, small protrusions, valley between large paddles and base of small protrusions) that will be discussed below is shown in Figure 1H.

To better visualize individual fiber cell morphologies and F-actin organization at different stages of maturation located at different depths in the lens, we developed a novel method to

Investigative Ophthalmology & Visual Science

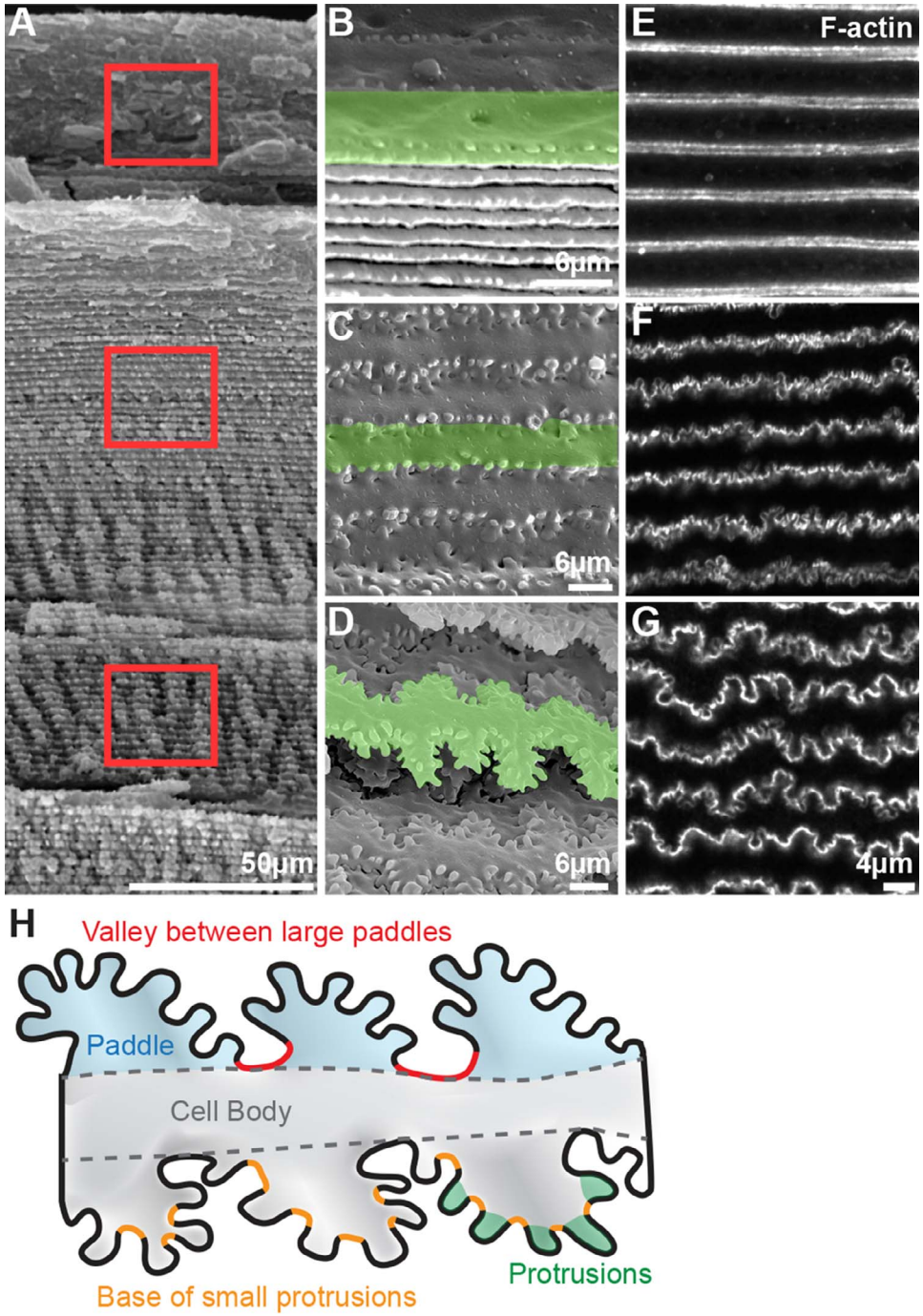

Figure 1. (**A–D**) Scanning electron microscopy (SEM) at various depths in 3-month-old wild-type (WT) lenses. *Boxed regions* in (**A**) indicate the approximate location where (**B–D**) higher-magnification images were obtained. (**B–D**) Cortical newly formed fiber cells (**B**) are straight, with balls and sockets along the broad sides and small protrusions along the vertices. As fiber cells differentiate (**C**), the cells remain straight and more small protrusions are formed along the cell vertices. Mature lens fibers (**D**) form large interlocking paddle domains decorated by small protrusions along the cell vertices. Single fibers are highlighted in *green* to show the changes in cell morphology as the fibers mature. Note that (**D**) is a different orientation of the same fiber cell shown in Figure 3B of Blankenship et al.[6] (**E–G**) Confocal fluorescence microscopy of phalloidin staining of fiber cells in 6-week-old *Tmod1*$^{+/+}$ lens fiber cell bundles (located at depths comparable to those in [**B–D**]) reveals that F-actin is enriched in large paddle domains and small interlocking protrusions at the vertices of fiber cells. (**H**) Diagram (not to scale) of mature lens fiber cells with large paddles (*light blue shading*), valleys between large paddles (*red lines*), small protrusions (*green shading*), and bases of small protrusions (*yellow lines*) along the short sides of the cell. *Scale bars*: 50 μm (**A**); 6 μm (**B–D**); 4 μm (**E–G**).

immunostain single lens fiber cells. Mouse lenses were microdissected, decapsulated, and fixed overnight at 4°C; and after fixation, lenses were cut into quarters and postfixed before immunostaining. Single fiber cells as well as fiber cell bundles spontaneously detached from the bulk lens quarters during the immunostaining process, and segments up to 200 μm long could be imaged by confocal microscopy. From our preparation, we observed three types of fiber cells: tightly

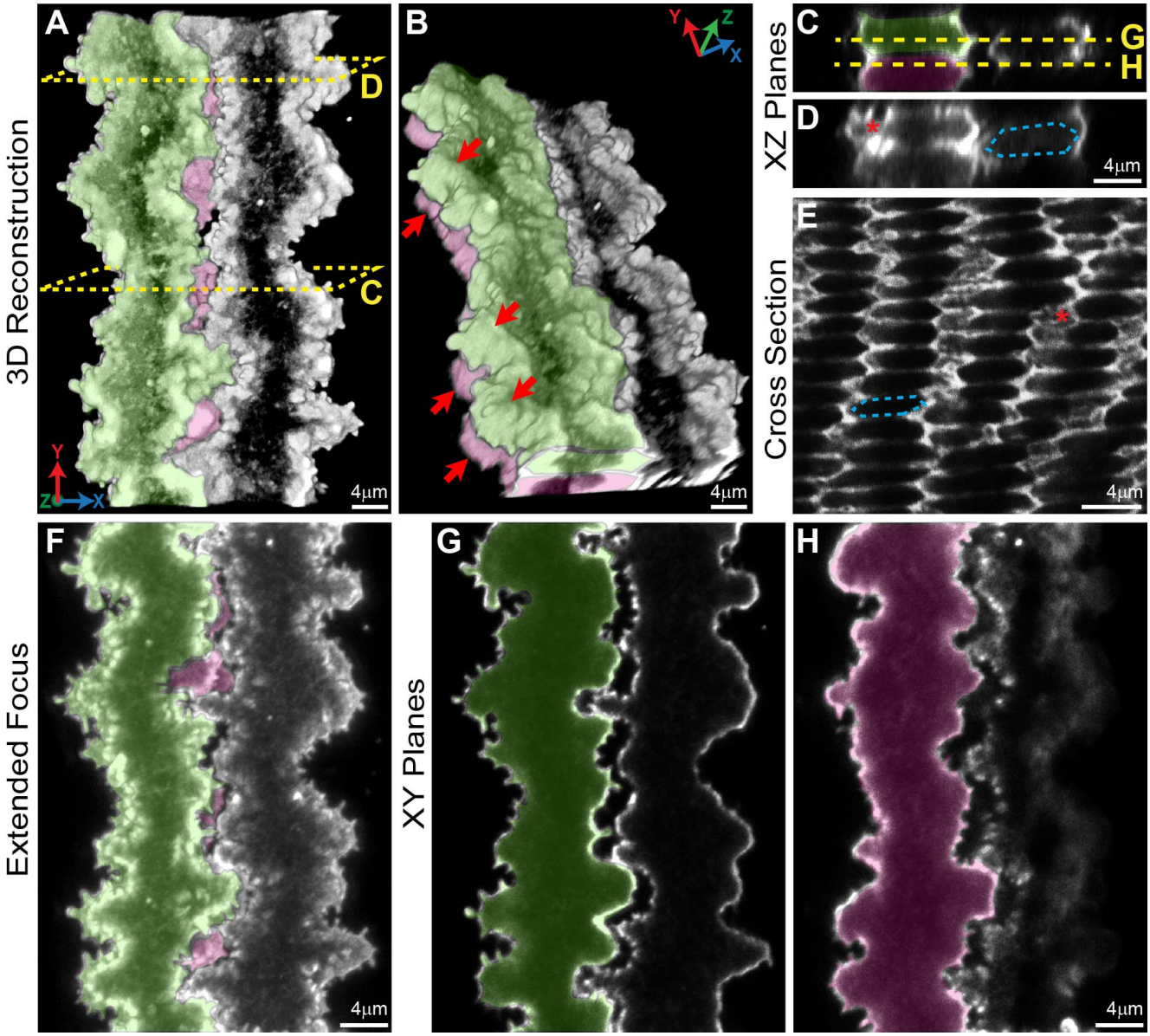

Figure 2. Confocal fluorescence microscopy images (2D single optical planes, extended focus flattened Z-stack, 3D reconstruction and cross section) of F-actin in neighboring mature fiber cells in 6-week-old *Tmod1*$^{+/+}$ lenses. Single fiber cells are pseudocolored *green* or *pink* or uncolored. 3D reconstruction of Z-stacks through three neighboring fibers shows interlocking structures between adjacent cells (**A**) and coordinated paddle domains between cells of neighboring layers (**B**) (*red arrows*). *Dashed boxes* show the level where single XZ planes in (**C**, **D**) are derived. A single 2D XZ plane from the 3D reconstruction shows normal hexagonal fiber cell morphology (**C**, **D**) (hexagonal cell body outlined with *blue dashed lines*) with paddles and protrusions along the short side (**D**) (*red asterisk*). The F-actin staining pattern in dissociated fiber cells is similar to what is typically observed in cross sections through hexagonal mature lens fibers that have undergone denucleation (**E**) (hexagonal cell body outlined with *blue dashed lines*), demonstrating enriched F-actin along the short sides of these fibers and in regions of paddles and protrusions (*red asterisk*) with less intense F-actin signals along the broad sides. Extended focus image of the flattened Z-stack shows F-actin–rich interlocking paddles decorated by small protrusions along the short sides of the cells, creating a 3D zipper between adjacent cells (**F**). Single XY optical sections along the anterior–posterior axis through the fiber cells (**G**, **H**), where the *dashed lines* are drawn through the XZ plane in (**C**) show interlocking domains between fibers with some separation between the cells. *Scale bars*: 4 μm.

apposed fiber cell bundles (Fig. 1), loosely dissociated lens fiber cell bundles (Fig. 2), and single lens fibers that are detached from neighboring cells (Figs. 3–7). Immunostaining of three neighboring fiber cell segments showed that F-actin is enriched in protrusions and paddles, and that the complex morphology of this ingenious 3D zipper is well preserved in these partially separated fibers (Fig. 2). Three-dimensional reconstruction of the lens fibers shows interlocking paddles and protrusions between adjacent cells (Fig. 2A) and alignment of paddle domains between cells of neighboring layers (Fig. 2B, red arrows, green and pink cells). While difficult to visualize in these images, each fiber cell has three sets of coordinated paddles and protrusions along the short sides, corresponding to the three vertices located on the short sides.[6,9,10,13] Two-dimensional (2D) projections of single XZ planes reveal normal hexagonal fiber cell shapes with

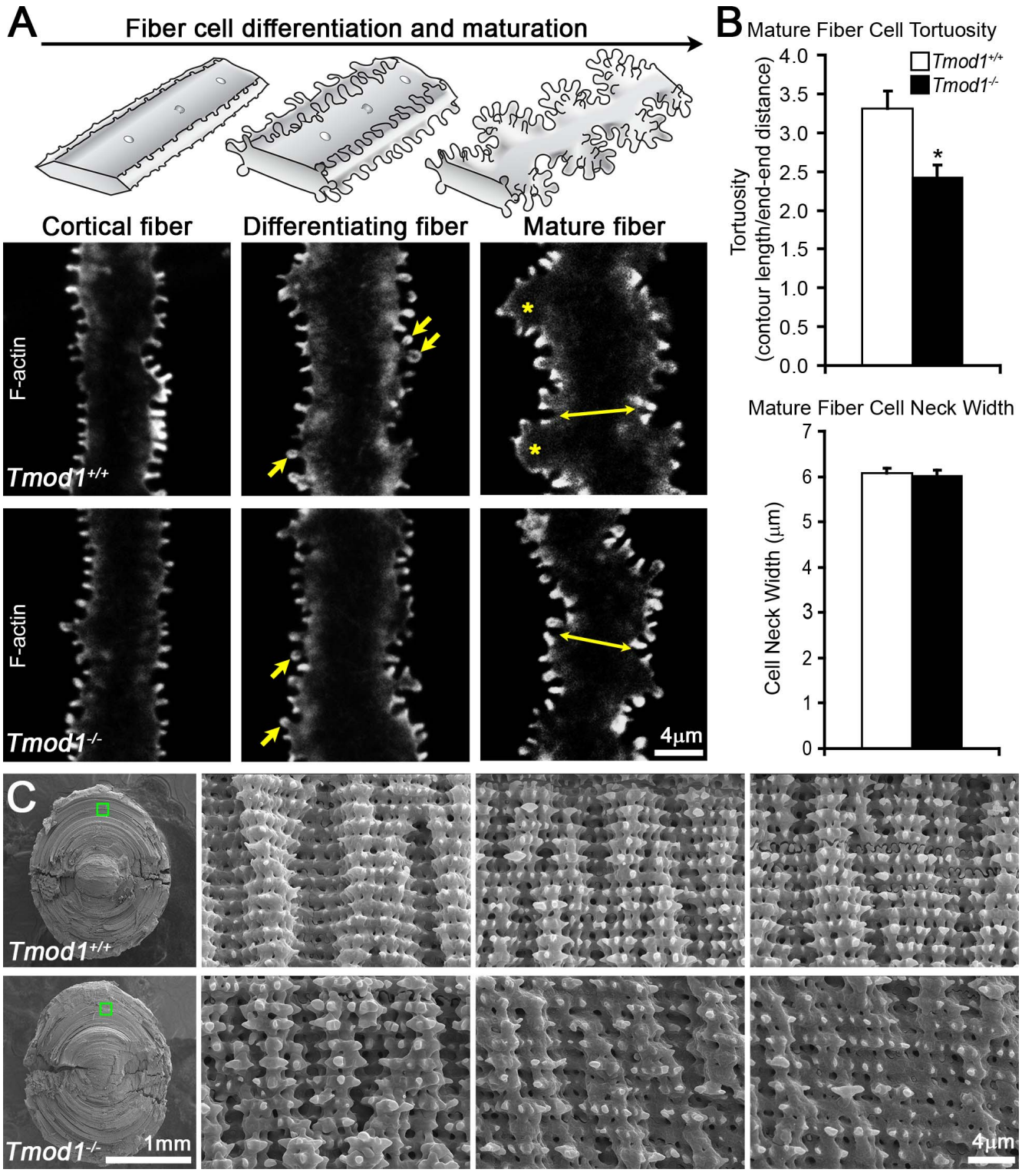

Figure 3. Confocal fluorescence microscopy images (2D, single optical plane) of F-actin in fiber cells at various depths and SEM in 6-week-old (**A**) and 2-month-old (**C**) *Tmod1*$^{+/+}$ and *Tmod1*$^{-/-}$ lenses. (**A**) Diagrams of normal cortical, differentiating, and mature fiber cells are shown along the *top*. *Tmod1*$^{+/+}$ and *Tmod1*$^{-/-}$ cortical and differentiating fiber cells are straight with small F-actin protrusions along their vertices. Protrusions in differentiating fibers have more pronounced head and neck regions (*arrows*). *Tmod1*$^{+/+}$ mature fibers have large paddle domains (*asterisks*) with F-actin–rich small protrusions, while *Tmod1*$^{-/-}$ fiber cells have F-actin–positive protrusions, but very few paddles. (**B**) *Tmod1*$^{-/-}$ mature fiber cells display a significant decrease in tortuosity ($n = 9$, $^*P < 0.01$), but the cell neck width was unaffected (*double-headed arrows* in [**A**]) between *Tmod1*$^{+/+}$ and *Tmod1*$^{-/-}$ lenses ($n = 9$). (**C**) Low-magnification SEM with *boxed regions* indicating the location of higher-magnification images. Comparable regions are identified by measuring outward from the nucleus at the center of the lens, since some peripheral cortical fibers are lost in the sample preparation procedure. *Tmod1*$^{+/+}$ lenses have rows of mature fiber cells with coordinated paddle protrusions that are decorated by smaller protrusions of equal size and spacing. In contrast, *Tmod1*$^{-/-}$ mature lens fibers have disorganized paddles with irregular protrusions. *Scale bars*: 4 μm (**A**); 1 mm (**C**) (low magnification *left*); 4 μm (**C**) (high magnification).

Investigative Ophthalmology & Visual Science

enriched F-actin along the short sides near vertices, and less intense F-actin staining along the broad sides (Figs. 2C, 2D, hexagonal cell body outlined with blue dashed lines). The XZ projection through the cell neck (Fig. 2C) shows smooth F-actin staining along the cell membrane, while the XZ projection through a region with paddles (Fig. 2D) reveals F-actin–rich regions of paddles and protrusions at their vertices (red asterisk). This is analogous to the view seen in a typical equatorial cross section through mature lens fibers that have undergone denucleation, ~150 to 200 μm from the lens capsule (Fig. 2E, hexagonal cell body outlined with blue dashed lines and paddles and protrusions indicated by a red asterisk). An extended focus image of the flattened Z-stack of the individual fiber cells clearly demonstrates the interlocking paddles and protrusions between adjacent cells (Fig. 2F). Single optical projections in the XY plane (Figs. 2G, 2H) reveal slight gaps between the interlocking domains of adjacent cells (green and white cells in Fig. 2G, pink and white cells in Fig. 2H). In favorable views of a fiber cell edge, F-actin appears more highly enriched in the small protrusions compared to paddles (Fig. 2G, far left edge of fiber cell). Note that due to the 3D nature of these complex interdigitations, single optical planes do not show all of the protrusions and paddles along the short sides of each cell. Our results indicate that our new immunostaining method for detached single fibers faithfully preserves fiber cell morphology observed in situ by SEM (Fig. 1), thus allowing detailed studies of the proteins required for the formation and/or stability of protrusions and paddles along fiber cell vertices.

Tmod1 Is Required for the Formation of Large Paddle Domains Between Mature Lens Fibers

To investigate whether the Tmod1-stablized actin cytoskeleton plays a role in the formation or stabilization of fiber cell interdigitations, we compared fiber cell morphologies and F-actin organization in single fiber cells from *Tmod1*$^{+/+}$ and *Tmod1*$^{-/-}$ lenses. We distinguished cortical, differentiating, and mature fiber segments by their unique morphologies (diagram in Fig. 3A) and by observing the location of the single fiber with respect to depth in the bulk lens quarter. Single optical sections reveal that F-actin is highly enriched at the fiber cell membrane and in small protrusions in all fiber cells from both *Tmod1*$^{+/+}$ and *Tmod1*$^{-/-}$ lenses, including cortical, differentiating, and mature single fibers (Fig. 3A). *Tmod1*$^{+/+}$ and *Tmod1*$^{-/-}$ cortical and differentiating fibers are straight with numerous small protrusions along their vertices, and no obvious differences in F-actin or in cell morphologies are observed. Protrusions along cortical fibers appear finger-like, while protrusions along differentiating fibers have more obvious head and neck regions (Fig. 3A, arrows). The *Tmod1*$^{+/+}$ mature fiber cell, which has undergone denucleation (~150–250 μm deep from the lens capsule), displays large paddle domains with small protrusions (Fig. 3A, asterisks) as seen above (Fig. 2). Unexpectedly, unlike cortical and differentiating fibers, which are not affected by absence of Tmod1, the *Tmod1*$^{-/-}$ mature fiber cell lacks normal paddles despite retaining an overall undulating shape with abundant F-actin–rich small protrusions. A useful metric to compare paddle formation between control and knockout mature fiber cells is the contour length of the fiber cell edge, or tortuosity, measured along the paddle contours relative to the overall fiber cell length. Indeed, *Tmod1*$^{-/-}$ mature fiber cells had a statistically significant decrease in tortuosity compared to *Tmod1*$^{+/+}$ mature fiber cells, consistent with a partial loss of large paddles (Fig. 3B). We also measured the cell neck width (Fig. 3A, double arrows; Fig. 3B) to ensure that cells from a similar depth were being compared between *Tmod1*$^{+/+}$ and *Tmod1*$^{-/-}$ lenses and showed that there was no difference in the cell neck width.

To validate the observations based on single fiber cell immunostaining, we visualized fiber cell edges by classic SEM of half lenses to determine whether the loss of Tmod1 affects lens fiber cell interdigitations and protrusion morphologies. This showed that *Tmod1*$^{+/+}$ mature lens fibers are characterized by coordinated large paddle domains decorated by evenly spaced and sized small protrusions (~0.5–1.5 μm), as expected (Fig. 3C).[9,10,12,13,20] Similar to immunostained single fiber cells, the *Tmod1*$^{-/-}$ mature lens fibers appear to have reduced paddles with irregularly sized and arranged smaller protrusions (Fig. 3C), although the shapes of whole individual fiber cells are difficult to assess in these SEM preparations.

Disruption of β2-Spectrin Localization in *Tmod1*$^{-/-}$ Mature Lens Fibers

The ability to immunostain and visualize individual mature lens fiber cells provides an opportunity to investigate the actin cytoskeleton composition of protrusions versus paddles, and how loss of Tmod1 and perturbations of actin-associated proteins could account for defective paddles but not small protrusions in *Tmod1*$^{-/-}$ mature fiber cells. We hypothesized that Tmod1 and a subset of actin-binding proteins (ABPs) would be associated with paddles but not small protrusions, and that loss of Tmod1 would affect paddle-associated ABPs but not protrusion-associated ABPs, illuminating mechanisms underlying paddle formation. First, we investigated locations of Tmod1 and β2-spectrin in *Tmod1*$^{+/+}$ mature lens fiber cells as compared to *Tmod1*$^{-/-}$ mature lens fibers by immunostaining and confocal microscopy. Z-stacks collected through single fibers were flattened to view and compare the morphology of *Tmod1*$^{+/+}$ versus *Tmod1*$^{-/-}$ cells (Fig. 4A). In the *Tmod1*$^{+/+}$ mature fiber, we observed that both Tmod1 and β2-spectrin were excluded from the small protrusions and instead tended to be located along the contours of the paddle domains, where both Tmod1 and β2-spectrin staining signals appeared in large bright puncta. We also observed small bright β2-spectrin puncta along the membrane of the broad sides (Fig. 4A, center of cell), consistent with lens cross-section staining data in our previous study.[30] In single optical sections through the cytoplasm of a *Tmod1*$^{+/+}$ mature fiber, bright Tmod1 and β2-spectrin puncta are located mainly in valleys between large paddle domains along the cell edges (i.e., regions of concave curvature) (Figs. 4B, 4D, arrows). In contrast, in the *Tmod1*$^{-/-}$ mature fiber cell with aberrant and attenuated paddle contours, the bright β2-spectrin puncta along cell edges are reduced in number and now mostly dispersed in the fiber cell cytoplasm, as seen in single optical sections through the middle of the cell (Fig. 4B, asterisks). A heat map of β2-spectrin fluorescence intensity shows increased cytoplasmic staining signals in the knockout mature fiber cell (Fig. 4C, asterisks). However, there were no obvious differences in the punctate β2-spectrin staining pattern along the broad sides of *Tmod1*$^{-/-}$ cells as compared to *Tmod1*$^{+/+}$ cells (Fig. 4A, center of cell). β2-spectrin puncta are also occasionally observed at the base of the F-actin–rich small protrusions along the short sides (at the vertices) of the *Tmod1*$^{+/+}$ and *Tmod1*$^{-/-}$ fibers (Figs. 4B, 4D, arrowheads). No changes in overall F-actin staining intensity or distribution were observed, mostly likely because absence of Tmod1 does not affect morphology of small protrusions where most of the F-actin is located (Fig. 2). The presence of both Tmod1 and β2-spectrin puncta in valleys between large paddles in *Tmod1*$^{+/+}$ fiber cells supports the hypothesis that Tmod1 plays a role in the formation or maintenance of large paddle domains by stabilizing a spectrin–actin network normally located in these domains in mature fiber cells.

Investigative Ophthalmology & Visual Science

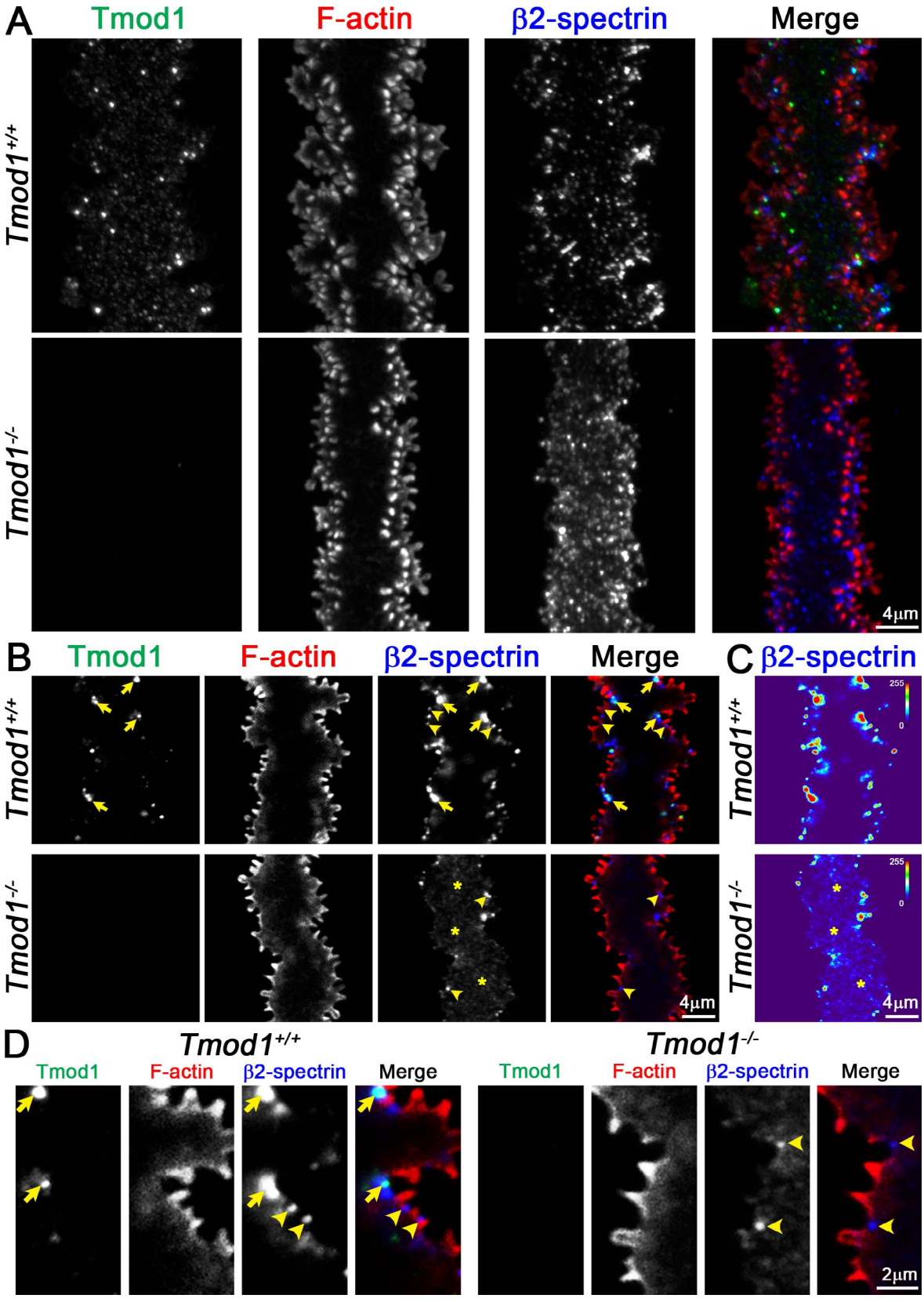

Figure 4. Immunostaining of single mature fiber cells from 6-week-old *Tmod1*$^{+/+}$ and *Tmod1*$^{-/-}$ lenses for Tmod1 (*green*), F-actin (*red*), and β2-spectrin (*blue*). (**A**) Extended focus of Z-stacks through mature fiber cells. The *Tmod1*$^{+/+}$ fiber has F-actin–rich large paddle domains and small protrusions along cell vertices. Tmod1 and β2-spectrin are enriched in numerous puncta in the control fiber cell. While the *Tmod1*$^{-/-}$ fiber has very few paddles, F-actin–rich small protrusions are still present. (**B**, **D**) Single optical section (2D) from a Z-stack, showing a section through the cytoplasm of the fiber cells, with enlargements. Tmod1 and β2-spectrin are enriched in puncta near the cell membrane in valleys between large

Investigative Ophthalmology & Visual Science

paddle domains in the *Tmod1*$^{+/+}$ fiber (*arrows*), and β2-spectrin is also enriched at the base of small protrusions in *Tmod1*$^{+/+}$ and *Tmod1*$^{-/-}$ fibers (*arrowheads*). The β2-spectrin staining signal appears diffuse and cytoplasmic (*asterisks*) with fewer membrane-associated puncta in the *Tmod1*$^{-/-}$ fiber. (**C**) Fluorescence intensity heat maps of β2-spectrin staining in *Tmod1*$^{+/+}$ and *Tmod1*$^{-/-}$ lens fibers show that β2-spectrin staining is more cytoplasmic (*asterisks*) in the *Tmod1*$^{-/-}$ fiber. *Scale bars*: 4 μm (**A–C**); 2 μm (**D**).

Moreover, alterations in β2-spectrin puncta locations and distributions in *Tmod1*$^{-/-}$ mature fibers are consistent with our previous results showing that the loss of Tmod1 perturbs the spectrin network in lens fiber cells.[30]

α-Actinin–Crosslinked Actin Filament Bundles Are Differentially Localized and Rearranged in *Tmod1*$^{-/-}$ Mature Fiber Cells

Our new data show that Tmod1 controls the morphology of large paddle domains in mature lens fibers, via stabilization of β2-spectrin associations at the base of paddle domains. These domains form the vertices between mature fiber cells visualized in lens cross sections and are associated with other ABPs, such as α-actinin,[41,42] Arp3,[43] and ezrin.[44,45] Therefore, we investigated whether these ABPs are located in the small protrusions or large paddles and whether they are disrupted in *Tmod1*$^{-/-}$ fibers. In mouse lenses, nonmuscle α-actinin (Actn1), a crosslinking protein for antiparallel actin filaments, has little or no staining signal in the cortical differentiating fibers, but is enriched at the short sides of mature fibers in a punctate pattern (Fig. 5A). In individual fiber cells, bright Tmod1 and α-actinin puncta are colocalized in valleys between large paddles in the mature *Tmod1*$^{+/+}$ lens fiber (Figs. 5B, 5C, arrows), while in the absence of Tmod1, α-actinin is distributed discontinuously along the entire cell membrane, even in regions with the abnormal and attenuated paddles. Careful examination of the α-actinin–F-actin merged image reveals that the α-actinin staining is now located at the bases of all the small protrusions (Fig. 5C, arrowheads). We performed Western blotting on soluble and insoluble lens protein samples to determine whether there was an increase in α-actinin protein levels in knockout lenses. We found no change in the amount of α-actinin in *Tmod1*$^{-/-}$ lenses compared to the control (data not shown). These data suggest that in control fiber cells, Tmod1 may restrict assembly of α-actinin–F-actin antiparallel bundles to the valleys between large paddles, promoting paddle morphogenesis. By contrast, in the absence of Tmod1, there may be a global rearrangement of the F-actin,[30] with increased α-actinin on the membrane.

Ezrin and Fimbrin Are Differentially Localized in Mature Fiber Cells, but Remain Unchanged in Absence of *Tmod1*

Next, we immunostained lenses for ezrin, which links F-actin networks to the plasma membrane[46] and fimbrin (aka plastin), a small crosslinker that bundles F-actin in a parallel orientation.[47] Similar to previous reports,[44,45,48] ezrin was detected only in lens fibers, where it was enriched on the short sides of cortical fibers, especially at vertices, with more uniform membrane staining in mature lens fibers as visualized in cross sections (Fig. 6A). In *Tmod1*$^{+/+}$ lens cross sections, fimbrin was present in epithelial cells and was also associated with the membranes of both differentiating and mature fiber cells (Fig. 6B). In preparations of single mature fiber cells, ezrin staining was continuous and colocalized with F-actin along the cell membrane in both *Tmod1*$^{+/+}$ and *Tmod1*$^{-/-}$ mature lens fibers (Fig. 6C). Ezrin also appeared to be enriched at the base of small protrusions as well as in the valleys between large paddles (Fig. 6D, arrowheads). On the other hand, fimbrin was restricted to puncta at the base of small protrusions in both control and knockout cells (Figs. 6C, 6D, arrows) and was not enriched in the valleys between large paddles, unlike Tmod1, β2-spectrin, and α-actinin. Neither ezrin nor fimbrin displayed any significant changes in the absence of Tmod1, suggesting that these F-actin networks are independent of Tmod1.

Arp3-Driven Branched Actin Networks May Play Roles in the Formation of Small Protrusions and Large Paddles

Previous work hypothesized that Arp2/3 may drive actin filament branching to push protrusions out of fiber cell membranes, while a pulling force on the membrane may be mediated by clathrin complexes along the membrane of the neighboring fiber.[20] Arp2/3 initiates branched actin filament assembly from preexisting filaments, and activation of Arp2/3 by WASP/WAVE family members and cortactin drives cadherin-directed actin assembly.[49–53] We previously demonstrated that Arp3 was enriched at the vertices of cortical fiber cells visualized in cross sections where it colocalized with N-cadherin.[43] However, Arp3 localization was not investigated in mature fibers, and thus we localized Arp3 and N-cadherin in single mature fibers. Arp3 was enriched in puncta at the base of the small F-actin–rich protrusions in both control and knockout mature fibers (Fig. 7, arrows), and Arp3 puncta were also found in valleys between large paddles in the *Tmod1*$^{+/+}$ fiber (Fig. 7, arrowheads). Low-intensity Arp3 staining can also be observed to extend into and fill small protrusions in both control and knockout fibers (Fig. 7B, open triangles). N-cadherin staining signal was predominantly at the cell membrane with a discontinuous pattern in control and knockout cells (Figs. 7A, 7B). This staining pattern is consistent with a recent study showing N-cadherin staining at the membranes in lens fiber cell bundles.[28] We also observed that Arp3 puncta at the base of small protrusions often coincide with areas of enriched N-cadherin staining (Fig. 7B, arrows). These observations would be consistent with the original hypothesis that Arp3 and N-cadherin play a role in assembly of the small F-actin–rich protrusions in fiber cells. However, since loss of Tmod1 does not greatly affect formation of small F-actin protrusions (Figs. 3–7) nor alter Arp3 or N-cadherin localization, fiber cell F-actin networks regulated by Arp3 or N-cadherin do not appear to be associated with the Tmod1-regulated F-actin networks that control paddle domain morphology.

Discussion

We have developed a novel technique to immunostain single lens fiber cells while preserving their complex morphology; this new method has allowed us to conduct detailed investigations of the F-actin structures and ABPs required for the formation of the interdigitations at fiber cell vertices. Our study has shown that Tmod1 is required for the formation of large paddles, but not small protrusions, between mature lens fiber cells. *Tmod1*$^{-/-}$ lens fibers undulate, but do not form coordinated paddle domains (Fig. 8A). These subtle changes in fiber cell morphology are correlated with decreased stiffness in *Tmod1*$^{-/-}$ lenses at low mechanical loads,[30] providing the first evidence for the hypothesis that fiber cell interdigitations influence lens mechanical integrity. By contrast, the *Tmod1*$^{-/-}$

Investigative Ophthalmology & Visual Science

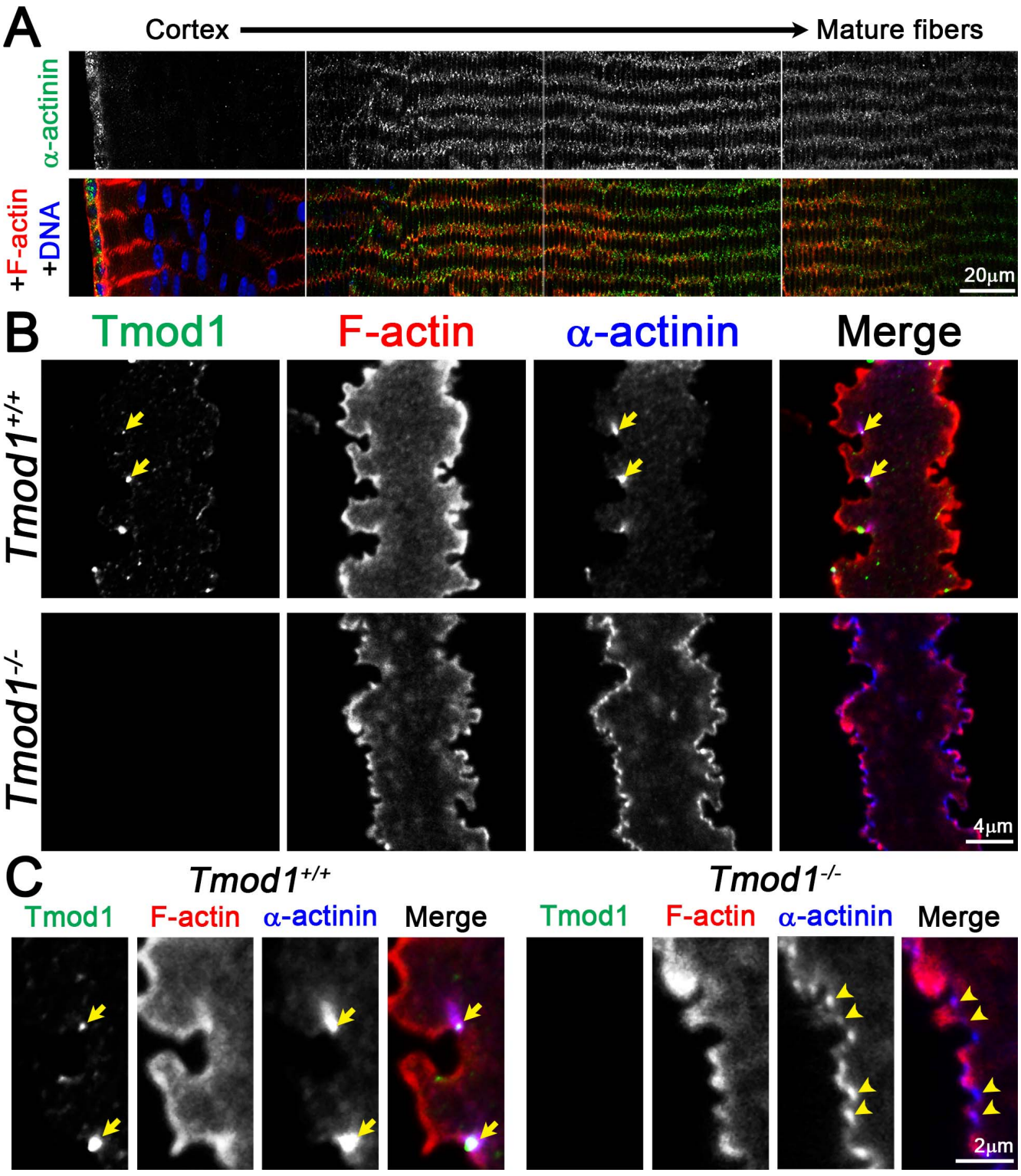

Figure 5. (**A**) Immunostaining of frozen lens section from 6-week-old *Tmod1*$^{+/+}$ mice for α-actinin (*green*) and F-actin (*red*). α-Actinin is present in epithelial cells with increased signal in maturing fiber cells. The staining signal is enriched on the short sides of mature fiber cells with a punctate pattern. (**B**, **C**) Immunostaining of single mature fiber cells (2D, single optical plane) from 6-week-old *Tmod1*$^{+/+}$ and *Tmod1*$^{-/-}$ lenses for Tmod1 (*green*), F-actin (*red*), and α-actinin (*blue*). Similar to Tmod1 and β2-spectrin, α-actinin is enriched in large puncta in valleys between large paddle domains in the *Tmod1*$^{+/+}$ fiber (*arrows* in [**B**, **C**]). In the *Tmod1*$^{-/-}$ fiber, α-actinin is present along the entire cell membrane. Enlargement shows that α-actinin is enriched near the base of small protrusions in the *Tmod1*$^{-/-}$ mature fiber cell (*arrowheads* in [**C**]). *Scale bars*: 20 μm (**A**); 4 μm (**B**); 2 μm (**C**).

Investigative Ophthalmology & Visual Science

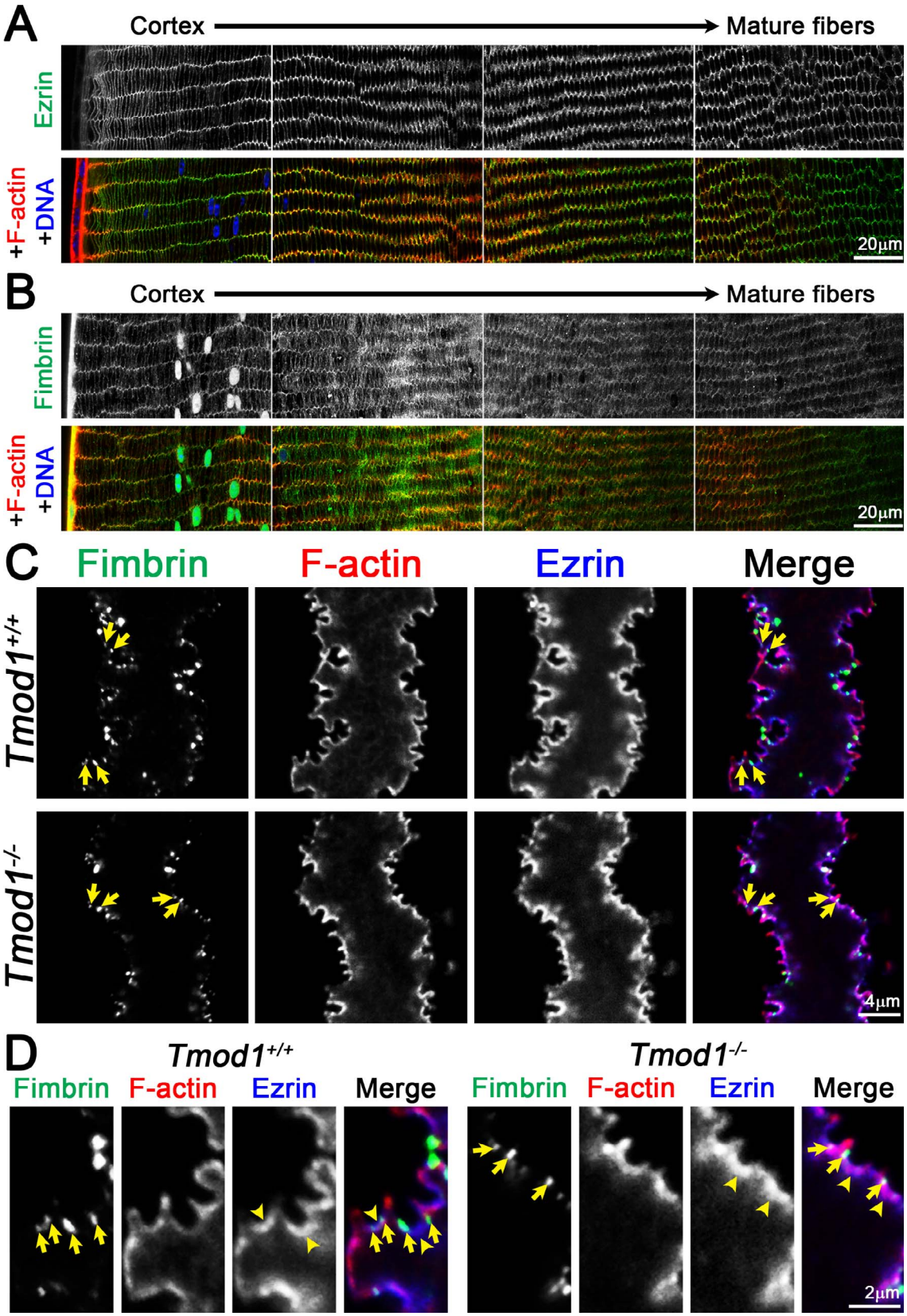

Figure 6. (**A**) Immunostaining of frozen lens section from 6-week-old *Tmod1*$^{+/+}$ mice for ezrin (*green*) and F-actin (*red*). Ezrin is present along the membranes of lens fiber cells and enriched at the vertices of cortical fibers and along the short sides of mature fiber cells. (**B**) Immunostaining of frozen lens section from 6-week-old *Tmod1*$^{+/+}$ mice for fimbrin (*green*) and F-actin (*red*). Fimbrin is present in epithelial and fiber cells. In fiber cells, fimbrin is distributed along the membrane in differentiating and mature fiber cells. (**C**, **D**) Immunostaining of single mature fiber cells (2D, single optical plane) from 6-week-old *Tmod1*$^{+/+}$ and *Tmod1*$^{-/-}$ lenses for fimbrin (*green*), F-actin (*red*), and ezrin (*blue*). As expected, ezrin

Investigative Ophthalmology & Visual Science

colocalizes with F-actin along the cell membrane and in interdigitations of *Tmod1*$^{+/+}$ and *Tmod1*$^{-/-}$ fibers. Interestingly, fimbrin is enriched in puncta near the base of small interlocking protrusions in *Tmod1*$^{+/+}$ and *Tmod1*$^{-/-}$ fibers (*arrows* in [**C**, **D**]). Enlargements show ezrin enrichment (*arrowheads* in [**D**]) at the base of small protrusions. *Scale bars*: 20 μm (**A**, **B**); 4 μm (**C**); 2 μm (**D**).

lenses with reduced paddle domains between mature lens fibers remain transparent, indicating that formation of large paddles is not required for lens transparency.[30] While recent studies have suggested that Aqp0 or ephrin-A5 may be important for normal fiber cell interdigitations,[7,28] *Aqp0*$^{-/-}$ and mixed-background *Efna5*$^{-/-}$ lenses have severe cataract phenotypes with fiber cell degeneration, which complicates interpretations and impedes further studies. Fortunately, the very mild phenotype in *Tmod1*$^{-/-}$ lenses has given us an opportunity to dissect the mechanisms underlying the formation of small protrusions as compared to large paddles located at the vertices of mature lens fiber cells.

Our novel immunostaining protocol for single fiber cells has yielded a wealth of new information about the proteins that control F-actin organization in small protrusions and in large paddles at the vertices of lens fiber cells (Fig. 8B). Tmod1 and the spectrin–actin network clearly play a key role in the formation and/or maintenance of the large paddle domains in mature lens fibers. Abnormal cytosolic localization of β2-spectrin in knockout single fibers extends our previous work showing that loss of Tmod1 leads to disruptions in the lens fiber membrane skeleton by providing a molecular mechanism connecting the F-actin cytoskeleton to fiber cell morphology.[30,31] Unlike loss of Tmod1 alone, which leads to selective

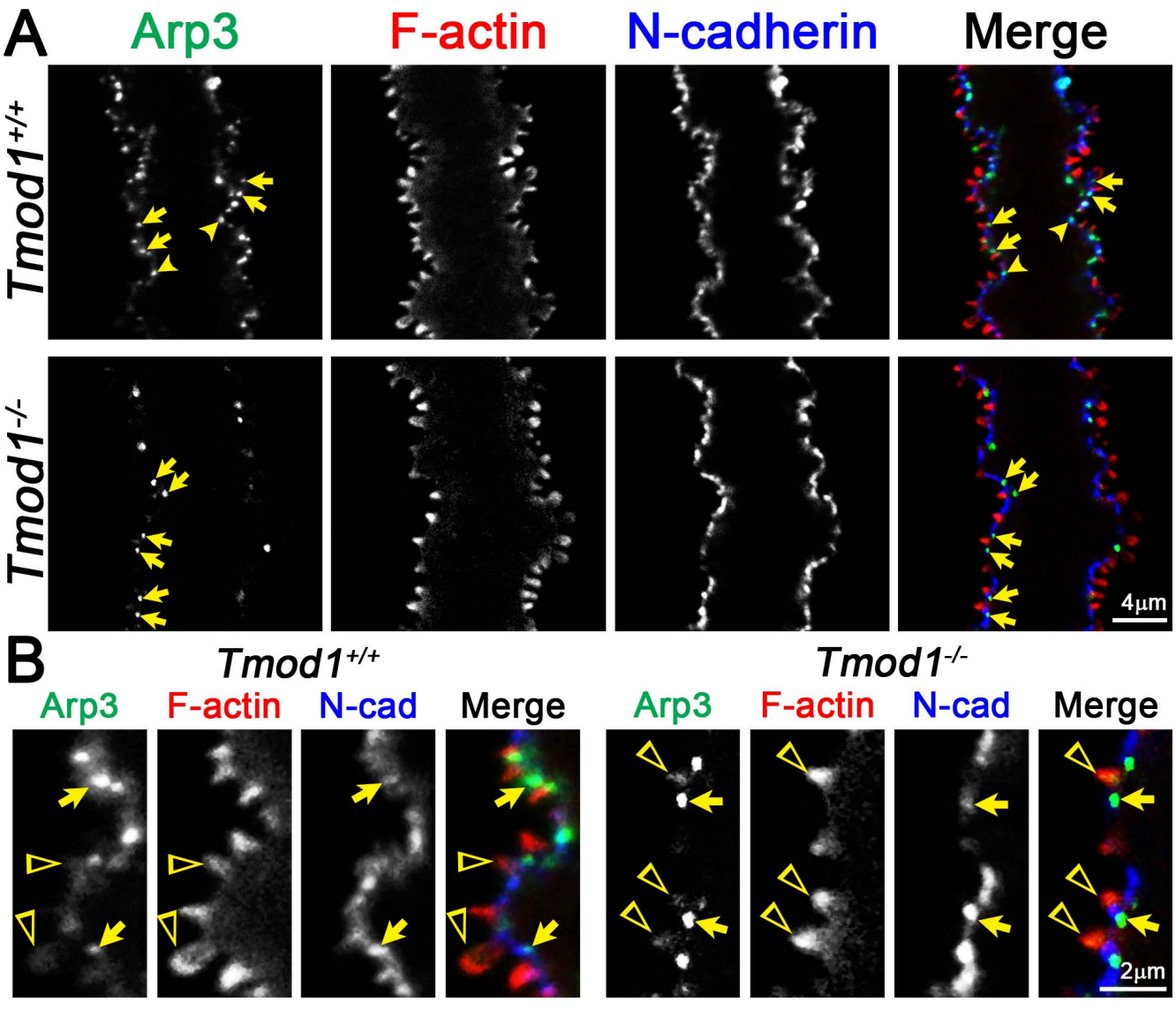

Figure 7. Immunostaining of single mature fiber cells (2D, single optical plane) from 6-week-old *Tmod1*$^{+/+}$ and *Tmod1*$^{-/-}$ lenses for Arp3 (*green*), F-actin (*red*), and N-cadherin (*blue*). (**A**) N-cadherin is localized along the cell membrane in *Tmod1*$^{+/+}$ and *Tmod1*$^{-/-}$ fibers and appears enriched along the base of protrusions and valleys between large paddles. Arp3 is enriched in puncta (*arrows*) near the base of small interlocking protrusions (*arrows*) in *Tmod1*$^{+/+}$ and *Tmod1*$^{-/-}$ fibers. Arp3 is also found in valleys between large paddles in the *Tmod1*$^{+/+}$ fiber (*arrowheads*). (**B**) Enlargements show that weak Arp3 staining extends into small protrusions (*open triangles*) in *Tmod1*$^{+/+}$ and *Tmod1*$^{-/-}$ fibers. Arp3 puncta at the base of small protrusions are often accompanied by enriched N-cadherin staining (*arrows*). *Scale bars*: 4 μm (**A**); 2 μm (**B**).

Investigative Ophthalmology & Visual Science

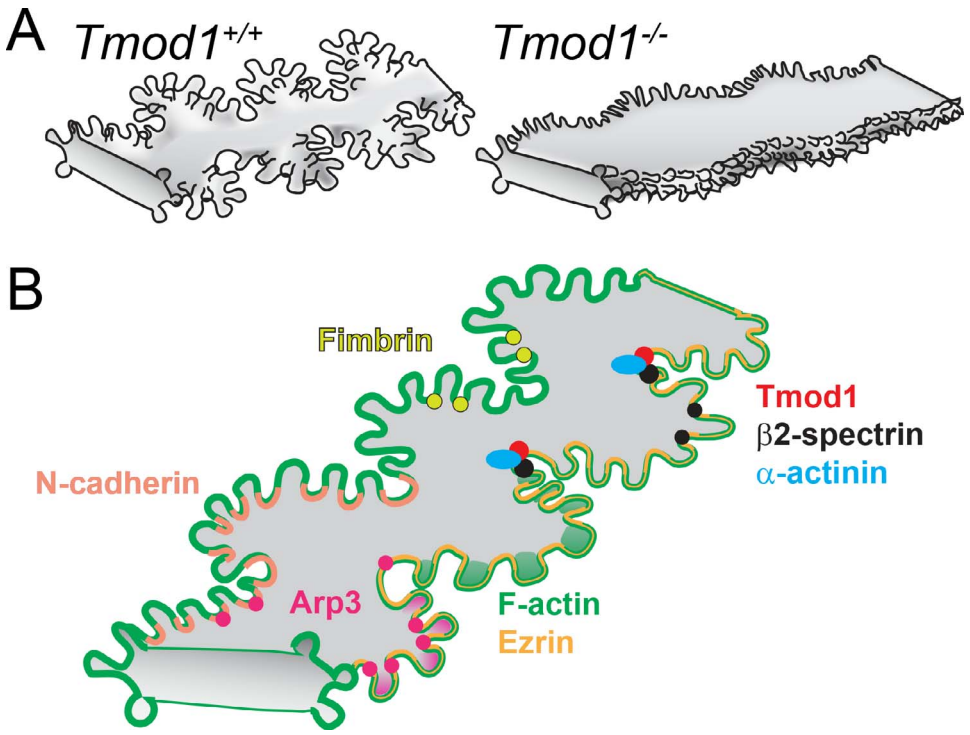

Figure 8. (**A**) During fiber cell maturation, large paddle domains with small interlocking protrusions form along the vertices of hexagonal fiber cells. Tmod1 is required for normal formation of large paddles between mature fiber cells. (**B**) Tmod1 may stabilize the F-actin–spectrin network as well as α-actinin–crosslinked antiparallel F-actin bundles in valleys between large paddles to maintain their structure. Formation of small protrusions may be facilitated by Arp3-nucleated actin networks, and fimbrin-crosslinked parallel F-actin bundles at the base of protrusions, while ezrin may stabilize actin networks along the entire fiber cell membrane and N-cadherin promotes cell–cell interactions.

reduction of large paddle domains, we showed previously that combined loss of Tmod1 and CP49, a beaded intermediate filament protein, leads to reduction in small protrusions at the vertices of mature fiber cells,[31] suggesting that both actin and intermediate filaments are needed for normal formation or stabilization of these smaller interdigitations.

Interestingly, α-actinin is also found in foci in the valleys between large paddles where it colocalizes with Tmod1 in mature *Tmod1*$^{+/+}$ fiber cells, suggesting that Tmod1 may cap the pointed ends of actin filaments crosslinked by spectrin and/or α-actinin. α-Actinin belongs to a protein family that includes spectrin, dystrophin, and utrophin,[54,55] and α-actinin–crosslinked F-actin bundles can interact with myosin II to generate contractile forces.[56] It is possible that α-actinin–bundled F-actin interacts with myosin II to generate force to push and/or pull the fiber cell membrane to create the large paddles. Strikingly, in *Tmod1*$^{-/-}$ mature fiber cells, the α-actinin staining signal becomes more broadly localized along the fiber cell membrane in between the small protrusions. However, similar to β2-spectrin,[30] we observe changes in the localization of α-actinin without changes in the protein level. This implies that α-actinin may be restricted to Tmod1-capped F-actin in wild-type cells but become aberrantly distributed and abnormally crosslink other F-actin populations in the absence of Tmod1. Since *Tmod1*$^{-/-}$ lenses have reduced levels of tropomyosin (TM),[30] a stabilizing protein that binds along the side of F-actin and enhances Tmod1 capping of actin pointed ends,[57–59] and TM inhibits α-actinin binding to F-actin,[60] additional F-actin binding sites may now be available in knockout lens fibers for α-actinin binding. It may also be significant that the localization of α-actinin in the *Tmod1*$^{-/-}$ mature fiber cell resembles that of N-cadherin in the *Tmod1*$^{-/-}$ mature fiber cell. This suggests the possibility that expansion of α-actinin–crosslinked F-actin networks at N-cadherin–mediated cell–cell junctions may partially compensate for loss of spectrin–actin networks, perhaps as a mechanical response, albeit being unable to assist fiber cells in forming large paddle domains. Our data in the lens parallel abnormal α-actinin and F-actin staining patterns in *Tmod1*$^{-/-}$ embryonic heart muscle cells that fail to assemble myofibrils.[61] Further studies will be needed to define the interactions between Tmod1 and α-actinin–associated F-actin, as well as the changes in α-actinin and actin binding in the absence of Tmod1.

This work also provides the first evidence that distinct ABPs may selectively control the formation of small protrusions as compared to large paddles in lens fiber cells. In addition to intestinal microvilli,[62,63] fimbrin has been found in protrusions in other cell types, including stereocilia of the inner ear hair cells[64–68] and microvilli of photoreceptors,[69] taste receptor cells,[70] nasal epithelial cells,[71] and respiratory brush cells.[72,73] The location of fimbrin in puncta at the base, but not throughout the small F-actin–rich protrusions in single mature fiber cells, suggests that these structures are not analogous to the microvilli of other cells, where fimbrin is present along their entire length. Instead, fimbrin crosslinking of F-actin into rigid parallel filament bundles[74] may help in stabilizing the small protrusions at their bases. Our data are also consistent with previous studies showing that the presence of fimbrin and α-actinin is mutually exclusive due to the different spacings between F-actins when bundled by fimbrin or α-actinin.[75–77]

While fimbrin is found in small puncta at the base of the small protrusions in mature fiber cells, ezrin is associated with F-actin along the entire membrane of mature fiber cells, including along the membranes of small protrusions. Ezrin–radixin–moesin (ERM) proteins link actin filament networks to the plasma membrane.[46] Immunoprecipitation experiments have shown that an actin anchorage complex consisting of ezrin–periplakin–periaxin–desmoyokin (EPPD) proteins is as-

sociated with moesin, spectrin, and plectin in the lens, suggesting an interaction between ERM, EPPD, and the spectrin–actin networks.[44] Decreased actin and spectrin protein levels and fiber cell membrane staining signals are observed in periaxin knockout lenses, further indicating that the EPPD complexes may function to stabilize the spectrin–actin membrane skeleton.[48,78]

Our work strengthens the hypothesis that Arp2/3 may drive the formation of small protrusions by nucleating branched F-actin networks.[20] We had expected Arp3 to be enriched with F-actin within the small protrusions; instead, we found that Arp3 is predominantly enriched in bright puncta at the base of small protrusions, although dim, diffuse Arp3 staining can be detected extending into small protrusions. This suggests that Arp2/3 nucleation of branched F-actin networks occurs predominantly near the cell membrane at the base of protrusions and paddles, and to a lesser extent within the body of the protrusion, as originally proposed.[20] Notably, location of Arp3 at the base of small protrusions where N-cadherin is also located implies that Arp2/3 may nucleate F-actin in N-cadherin cell contacts, as previously shown for E-cadherin at cell junctions in epithelial cells.[79,80] Since Arp3 staining is comparable between *Tmod1*$^{+/+}$ and *Tmod1*$^{-/-}$ mature lens fibers, Tmod1 does not control Arp2/3-driven F-actin branching, which is thus unlikely to play a role in formation or maintenance of the large paddle contours in mature lens fibers.

We observe that Tmod1, β2-spectrin, α-actinin, fimbrin, and Arp3 are localized to small puncta at the base of some but not all protrusions and/or paddles in mature fiber cells. There are several possible reasons why proteins are not consistently localized to all protrusions and/or paddles. First, since the protrusions and paddles are complex 3D structures, confocal imaging of single optical sections (as presented here) may miss staining signals from out-of-plane structures. Second, our fixation conditions may lead to variable epitope accessibility in the case of proteins that are components of dense F-actin cytoskeletal structures. Third, preparation of single fiber cells that dissociates fibers from tightly adhered neighboring cells may lead to small rips and tears along the membrane, leading to a loss in staining at some protrusions and paddles. However, based on staining of single fibers with wheat germ agglutinin (data not shown), plasma membrane continuity does not appear to be compromised by our preparation method. Finally, fourth, it is attractive to speculate that constant membrane remodeling occurs in lens fiber cells during differentiation and maturation, requiring dynamic changes in the actin cytoskeleton. This notion is supported by the presence of a pool of monomeric G-actin in the lens,[31,81] consistent with ongoing F-actin polymerization and depolymerization in fiber cells. Actin cytoskeleton reorganization is a hallmark of normal lens fiber differentiation,[31,43] and there is an increase in polymerized F-actin versus monomeric G-actin in newly formed lens fibers.[82] Since our staining experiments capture a single snapshot in time of protein localization, we miss the dynamic changes that may remodel the membrane.

In summary, we have developed a novel technique to immunostain single lens fiber cells and have shown that Tmod1 stabilizes the spectrin–actin network and α-actinin–crosslinked antiparallel F-actin bundles in the valleys between large paddles to maintain their structure. On the other hand, formation of small protrusions is likely facilitated by Arp3-nucleated actin networks, as well as fimbrin-crosslinked parallel F-actin bundles, which do not depend on Tmod1. Thus, this work reveals specific ABPs required for the formation of large paddles between lens fibers, and suggests that large paddles between mature fiber cells are needed for lens mechanical integrity.

Acknowledgments

Supported by National Eye Institute Grants R01 EY017724 (VMF and subcontract to W-KL), R01 EY05314 (W-KL), and R01 EY08747 (PGF).

Disclosure: **C. Cheng**, None; **R.B. Nowak**, None; **S.K. Biswas**, None; **W.-K. Lo**, None; **P.G. FitzGerald**, None; **V.M. Fowler**, None

References

1. Lovicu FJ, Robinson ML. *Development of the Ocular Lens*. Cambridge, UK, New York: Cambridge University Press; 2004: xv, 398.
2. Kuszak JR, Zoltoski RK, Sivertson C. Fibre cell organization in crystalline lenses. *Exp Eye Res*. 2004;78:673–687.
3. Kuszak JR, Mazurkiewicz M, Jison L, Madurski A, Ngando A, Zoltoski RK. Quantitative analysis of animal model lens anatomy: accommodative range is related to fiber structure and organization. *Vet Ophthalmol*. 2006;9:266–280.
4. Piatigorsky J. Lens differentiation in vertebrates. A review of cellular and molecular features. *Differentiation*. 1981;19:134–153.
5. Bassnett S. On the mechanism of organelle degradation in the vertebrate lens. *Exp Eye Res*. 2009;88:133–139.
6. Blankenship T, Bradshaw L, Shibata B, Fitzgerald P. Structural specializations emerging late in mouse lens fiber cell differentiation. *Invest Ophthalmol Vis Sci*. 2007;48:3269–3276.
7. Lo WK, Biswas SK, Brako L, Shiels A, Gu S, Jiang JX. Aquaporin-0 targets interlocking domains to control the integrity and transparency of the eye lens. *Invest Ophthalmol Vis Sci*. 2014;55:1202–1212.
8. Kuwabara T. The maturation of the lens cell: a morphologic study. *Exp Eye Res*. 1975;20:427–443.
9. Willekens B, Vrensen G. The three-dimensional organization of lens fibers in the rabbit. A scanning electron microscopic reinvestigation. *Albrecht Von Graefes Arch Klin Exp Ophthalmol*. 1981;216:275–289.
10. Willekens B, Vrensen G. The three-dimensional organization of lens fibers in the rhesus monkey. *Albrecht Von Graefes Arch Klin Exp Ophthalmol*. 1982;219:112–120.
11. Kistler J, Gilbert K, Brooks HV, Jolly RD, Hopcroft DH, Bullivant S. Membrane interlocking domains in the lens. *Invest Ophthalmol Vis Sci*. 1986;27:1527–1534.
12. Kuszak J, Alcala J, Maisel H. The surface morphology of embryonic and adult chick lens-fiber cells. *Am J Anat*. 1980; 159:395–410.
13. Willekens B, Vrensen G. Lens fiber organization in four avian species: a scanning electron microscopic study. *Tissue Cell*. 1985;17:359–377.
14. Dickson DH, Crock GW. Interlocking patterns on primate lens fibers. *Invest Ophthalmol*. 1972;11:809–815.
15. Lo WK, Harding CV. Square arrays and their role in ridge formation in human lens fibers. *J Ultrastruct Res*. 1984;86: 228–245.
16. Biswas SK, Lee JE, Brako L, Jiang JX, Lo WK. Gap junctions are selectively associated with interlocking ball-and-sockets but not protrusions in the lens. *Mol Vis*. 2010;16:2328–2341.
17. Lo WK, Reese TS. Multiple structural types of gap junctions in mouse lens. *J Cell Sci*. 1993;106(pt 1):227–235.
18. Harding CV, Susan S, Murphy H. Scanning electron microscopy of the adult rabbit lens. *Ophthalmic Res*. 1976;8:443–455.
19. Leeson TS. Lens of the rat eye: an electron microscope and freeze-etch study. *Exp Eye Res*. 1971;11:78–82.
20. Zhou CJ, Lo WK. Association of clathrin, AP-2 adaptor and actin cytoskeleton with developing interlocking membrane domains of lens fibre cells. *Exp Eye Res*. 2003;77:423–432.

21. Kuszak JR, Macsai MS, Rae JL. Stereo scanning electron microscopy of the crystalline lens. *Scan Electron Microsc*. 1983;(pt 3):1415–1426.
22. Wang E, Geng A, Maniar AM, Mui BW, Gong X. Connexin 50 regulates surface ball-and-socket structures and fiber cell organization. *Invest Ophthalmol Vis Sci*. 2016;57:3039–3046.
23. Kirchhausen T. Adaptors for clathrin-mediated traffic. *Annu Rev Cell Dev Biol*. 1999;15:705–732.
24. Kirchhausen T. Clathrin. *Annu Rev Biochem*. 2000;69:699–727.
25. Kirchhausen T, Harrison SC, Heuser J. Configuration of clathrin trimers: evidence from electron microscopy. *J Ultrastruct Mol Struct Res*. 1986;94:199–208.
26. Pearse BM, Smith CJ, Owen DJ. Clathrin coat construction in endocytosis. *Curr Opin Struct Biol*. 2000;10:220–228.
27. Smith CJ, Pearse BM. Clathrin: anatomy of a coat protein. *Trends Cell Biol*. 1999;9:335–338.
28. Biswas S, Son A, Yu Q, Zhou R, Lo WK. Breakdown of interlocking domains may contribute to formation of membranous globules and lens opacity in ephrin-A5 mice. *Exp Eye Res*. 2015;145:130–139.
29. Yoon KH, Blankenship T, Shibata B, Fitzgerald PG. Resisting the effects of aging: a function for the fiber cell beaded filament. *Invest Ophthalmol Vis Sci*. 2008;49:1030–1036.
30. Gokhin DS, Nowak RB, Kim NE, et al. Tmod1 and CP49 synergize to control the fiber cell geometry, transparency, and mechanical stiffness of the mouse lens. *PLoS One*. 2012;7:e48734.
31. Nowak RB, Fischer RS, Zoltoski RK, Kuszak JR, Fowler VM. Tropomodulin1 is required for membrane skeleton organization and hexagonal geometry of fiber cells in the mouse lens. *J Cell Biol*. 2009;186:915–928.
32. Nowak RB, Fowler VM. Tropomodulin 1 constrains fiber cell geometry during elongation and maturation in the lens cortex. *J Histochem Cytochem*. 2012;60:414–427.
33. Gokhin DS, Lewis RA, McKeown CR, et al. Tropomodulin isoforms regulate thin filament pointed-end capping and skeletal muscle physiology. *J Cell Biol*. 2010;189:95–109.
34. McKeown CR, Nowak RB, Moyer J, Sussman MA, Fowler VM. Tropomodulin1 is required in the heart but not the yolk sac for mouse embryonic development. *Circ Res*. 2008;103:1241–1248.
35. Moyer JD, Nowak RB, Kim NE, et al. Tropomodulin 1-null mice have a mild spherocytic elliptocytosis with appearance of tropomodulin 3 in red blood cells and disruption of the membrane skeleton. *Blood*. 2010;116:2590–2599.
36. Simirskii VN, Lee RS, Wawrousek EF, Duncan MK. Inbred FVB/N mice are mutant at the cp49/Bfsp2 locus and lack beaded filament proteins in the lens. *Invest Ophthalmol Vis Sci*. 2006;47:4931–4934.
37. Alizadeh A, Clark J, Seeberger T, Hess J, Blankenship T, FitzGerald PG. Characterization of a mutation in the lens-specific CP49 in the 129 strain of mouse. *Invest Ophthalmol Vis Sci*. 2004;45:884–891.
38. Sandilands A, Wang X, Hutcheson AM, et al. Bfsp2 mutation found in mouse 129 strains causes the loss of CP49′ and induces vimentin-dependent changes in the lens fibre cell cytoskeleton. *Exp Eye Res*. 2004;78:875–889.
39. Correia I, Chu D, Chou YH, Goldman RD, Matsudaira P. Integrating the actin and vimentin cytoskeletons. adhesion-dependent formation of fimbrin-vimentin complexes in macrophages. *J Cell Biol*. 1999;146:831–842.
40. Dorner AA, Wegmann F, Butz S, et al. Coxsackievirus-adenovirus receptor (CAR) is essential for early embryonic cardiac development. *J Cell Sci*. 2005;118:3509–3521.
41. FitzGerald PG, Casselman J. Discrimination between the lens fiber cell 115 kd cytoskeletal protein and alpha-actinin. *Curr Eye Res*. 1990;9:873–882.
42. Lo WK, Shaw AP, Wen XJ. Actin filament bundles in cortical fiber cells of the rat lens. *Exp Eye Res*. 1997;65:691–701.
43. Leonard M, Zhang L, Zhai N, et al. Modulation of N-cadherin junctions and their role as epicenters of differentiation-specific actin regulation in the developing lens. *Dev Biol*. 2011;349:363–377.
44. Straub BK, Boda J, Kuhn C, et al. A novel cell-cell junction system: the cortex adhaerens mosaic of lens fiber cells. *J Cell Sci*. 2003;116:4985–4995.
45. Bagchi M, Katar M, Lo WK, Yost R, Hill C, Maisel H. ERM proteins of the lens. *J Cell Biochem*. 2004;92:626–630.
46. Bretscher A, Chambers D, Nguyen R, Reczek D. ERM-Merlin and EBP50 protein families in plasma membrane organization and function. *Annu Rev Cell Dev Biol*. 2000;16:113–143.
47. Delanote V, Vandekerckhove J, Gettemans J. Plastins: versatile modulators of actin organization in (patho)physiological cellular processes. *Acta Pharmacol Sin*. 2005;26:769–779.
48. Maddala R, Skiba NP, Lalane R III, Sherman DL, Brophy PJ, Rao PV. Periaxin is required for hexagonal geometry and membrane organization of mature lens fibers. *Dev Biol*. 2011;357:179–190.
49. Blanchoin L, Amann KJ, Higgs HN, Marchand JB, Kaiser DA, Pollard TD. Direct observation of dendritic actin filament networks nucleated by Arp2/3 complex and WASP/Scar proteins. *Nature*. 2000;404:1007–1011.
50. Higgs HN, Pollard TD. Regulation of actin filament network formation through ARP2/3 complex: activation by a diverse array of proteins. *Annu Rev Biochem*. 2001;70:649–676.
51. Mullins RD, Heuser JA, Pollard TD. The interaction of Arp2/3 complex with actin: nucleation, high affinity pointed end capping, and formation of branching networks of filaments. *Proc Natl Acad Sci U S A*. 1998;95:6181–6186.
52. Uruno T, Liu J, Zhang P, et al. Activation of Arp2/3 complex-mediated actin polymerization by cortactin. *Nat Cell Biol*. 2001;3:259–266.
53. Weaver AM, Karginov AV, Kinley AW, et al. Cortactin promotes and stabilizes Arp2/3-induced actin filament network formation. *Curr Biol*. 2001;11:370–374.
54. Otey CA, Carpen O. Alpha-actinin revisited: a fresh look at an old player. *Cell Motil Cytoskeleton*. 2004;58:104–111.
55. Broderick MJ, Winder SJ. Spectrin, alpha-actinin, and dystrophin. *Adv Protein Chem*. 2005;70:203–246.
56. Choi CK, Vicente-Manzanares M, Zareno J, Whitmore LA, Mogilner A, Horwitz AR. Actin and alpha-actinin orchestrate the assembly and maturation of nascent adhesions in a myosin II motor-independent manner. *Nat Cell Biol*. 2008;10:1039–1050.
57. Kostyukova AS, Hitchcock-DeGregori SE. Effect of the structure of the N terminus of tropomyosin on tropomodulin function. *J Biol Chem*. 2004;279:5066–5071.
58. Weber A, Pennise CR, Babcock GG, Fowler VM. Tropomodulin caps the pointed ends of actin filaments. *J Cell Biol*. 1994;127:1627–1635.
59. Weber A, Pennise CR, Fowler VM. Tropomodulin increases the critical concentration of barbed end-capped actin filaments by converting ADP.P(i)-actin to ADP-actin at all pointed filament ends. *J Biol Chem*. 1999;274:34637–34645.
60. Drabikowski W, Nonomura Y, Maruyama K. Effect of tropomyosin on the interaction between F-actin and the 6S component of alpha-actinin. *J Biochem*. 1968;63:761–765.
61. Fritz-Six KL, Cox PR, Fischer RS, et al. Aberrant myofibril assembly in tropomodulin1 null mice leads to aborted heart development and embryonic lethality. *J Cell Biol*. 2003;163:1033–1044.
62. Chafel MM, Shen W, Matsudaira P. Sequential expression and differential localization of I-, L-, and T-fimbrin during differentiation of the mouse intestine and yolk sac. *Dev Dyn*. 1995;203:141–151.

Investigative Ophthalmology & Visual Science

63. Matsudaira PT, Burgess DR. Identification and organization of the components in the isolated microvillus cytoskeleton. *J Cell Biol*. 1979;83:667–673.
64. Zine A, Hafidi A, Romand R. Fimbrin expression in the developing rat cochlea. *Hear Res*. 1995;87:165–169.
65. Bretscher A. Fimbrin is a cytoskeletal protein that crosslinks F-actin in vitro. *Proc Natl Acad Sci U S A*. 1981;78:6849–6853.
66. Slepecky N, Chamberlain SC. Immunoelectron microscopic and immunofluorescent localization of cytoskeletal and muscle-like contractile proteins in inner ear sensory hair cells. *Hear Res*. 1985;20:245–260.
67. Sobin A, Flock A. Immunohistochemical identification and localization of actin and fimbrin in vestibular hair cells in the normal guinea pig and in a strain of the waltzing guinea pig. *Acta Otolaryngol*. 1983;96:407–412.
68. Flock A, Bretscher A, Weber K. Immunohistochemical localization of several cytoskeletal proteins in inner ear sensory and supporting cells. *Hear Res*. 1982;7:75–89.
69. Hofer D, Drenckhahn D. Molecular heterogeneity of the actin filament cytoskeleton associated with microvilli of photoreceptors, Müller's glial cells and pigment epithelial cells of the retina. *Histochemistry*. 1993;99:29–35.
70. Hofer D, Drenckhahn D. Localisation of actin, villin, fimbrin, ezrin and ankyrin in rat taste receptor cells. *Histochem Cell Biol*. 1999;112:79–86.
71. Hofer D, Shin DW, Drenckhahn D. Identification of cytoskeletal markers for the different microvilli and cell types of the rat vomeronasal sensory epithelium. *J Neurocytol*. 2000;29:147–156.
72. Hofer D, Drenckhahn D. Cytoskeletal markers allowing discrimination between brush cells and other epithelial cells of the gut including enteroendocrine cells. *Histochem Cell Biol*. 1996;105:405–412.
73. Hofer D, Drenckhahn D. Identification of brush cells in the alimentary and respiratory system by antibodies to villin and fimbrin. *Histochemistry*. 1992;98:237–242.
74. Glenney JR Jr, Kaulfus P, Matsudaira P, Weber K. F-actin binding and bundling properties of fimbrin, a major cytoskeletal protein of microvillus core filaments. *J Biol Chem*. 1981; 256:9283–9288.
75. Alberts B. *Molecular Biology of the Cell*. 5th ed. New York: Garland Science; 2008.
76. Cooper GM, Hausman RE. *The Cell: A Molecular Approach*. 4th ed. Washington, DC, Sunderland, MA: ASM Press, Sinauer Associates. 2007; xix, 820.
77. Vignjevic D, Kojima S, Aratyn Y, Danciu O, Svitkina T, Borisy GG. Role of fascin in filopodial protrusion. *J Cell Biol*. 2006; 174:863–875.
78. Maddala R, Walters M, Brophy PJ, Bennett V, Rao PV. Ankyrin-B directs membrane tethering of periaxin and is required for maintenance of lens fiber cell hexagonal shape and mechanics. *Am J Physiol Cell Physiol*. 2016;310:C115–C126.
79. Kovacs EM, Goodwin M, Ali RG, Paterson AD, Yap AS. Cadherin-directed actin assembly: E-cadherin physically associates with the Arp2/3 complex to direct actin assembly in nascent adhesive contacts. *Curr Biol*. 2002;12:379–382.
80. Verma S, Shewan AM, Scott JA, et al. Arp2/3 activity is necessary for efficient formation of E-cadherin adhesive contacts. *J Biol Chem*. 2004;279:34062–34070.
81. Woo MK, Lee A, Fischer RS, Moyer J, Fowler VM. The lens membrane skeleton contains structures preferentially enriched in spectrin-actin or tropomodulin-actin complexes. *Cell Motil Cytoskeleton*. 2000;46:257–268.
82. Ramaekers FC, Boomkens TR, Bloemendal H. Cytoskeletal and contractile structures in bovine lens cell differentiation. *Exp Cell Res*. 1981;135:454–461.

Investigative Ophthalmology & Visual Science